ORIGINAL ARTICLE

CrossMark

Pilot study on renal magnetic resonance diffusion tensor imaging: are quantitative diffusion tensor imaging values useful in the evaluation of children with ureteropelvic junction obstruction?

Jorge Delgado[1] · Jeffrey I. Berman[1,2] · Carolina Maya[1] · Robert H. Carson[1] · Susan J. Back[1,2] · Kassa Darge[1,2]

Abstract

Background Ureteropelvic junction (UPJ) obstruction is a common cause of renal injury in children. Indications for surgery are still controversial. Currently, there is no threshold to differentiate patients with suspected UPJ obstruction requiring surgery from the ones that do not, or to predict renal outcome after surgery. Several studies have demonstrated that diffusion tensor imaging (DTI) results may correlate with microstructural changes in the kidneys.

Objective To evaluate the feasibility of using DTI to identify UPJ obstruction kidneys.

Materials and methods We analyzed functional MR urography (fMRU) with renal DTI (b=0 and b=400, 20 directions, 1.5 Tesla, no respiratory triggering) in 26 kidneys of 19 children (mean age: 6.15 years) by comparing 13 kidneys with UPJ obstruction configuration that underwent pyeloplasty following the fMRU, and 13 anatomically normal age- and gender-matched kidneys. DTI tractography was reconstructed using a fractional anisotropy threshold of 0.10 and an angle threshold of 55°. User-defined regions of interest (ROIs) of the renal parenchyma (excluding collecting system) were drawn to quantify DTI parameters: fractional anisotropy, apparent diffusion coefficient (ADC), track length and track volume. The failure rate was evaluated.

Results All DTI parameters changed with age; fractional anisotropy decreased ($P<0.032$). Track volume and track length increased ($P<0.05$). ADC increased with age in normal kidneys ($P<0.001$) but not in UPJ obstruction kidneys ($P=0.11$). After controlling for age, the fractional anisotropy (UPJ obstruction mean: 0.18, normal kidney mean: 0.21; $P=0.001$) and track length (UPJ obstruction mean: 11.9 mm, normal kidney mean: 15.4 mm; $P<0.001$) were lower in UPJ obstruction vs. normal kidneys. There was a trend toward a higher ADC in UPJ obstruction kidneys vs. normal kidneys ($P=0.062$). The failure rate in UPJ obstruction kidneys due to technical limitations of DTI was 13/26 (50%).

Conclusion We demonstrated that fractional anisotropy is lower in UPJ obstruction than in normal kidneys. It is necessary to improve this technique to increase the success rate and to perform more studies to evaluate if a decrease in fractional anisotropy can differentiate UPJ obstruction kidneys from hydronephrotic kidneys without UPJ obstruction.

Keywords Children · Diffusion tensor imaging · Magnetic resonance imaging · Magnetic resonance urography · Ureteropelvic junction obstruction · Urinary tract

✉ Jorge Delgado
jorge.delgado.londono@gmail.com; delgadoj@email.chop.edu

1 Department of Radiology,
The Children's Hospital of Philadelphia,
3401 Civic Center Blvd.,
Philadelphia, PA 19104, USA

2 Department of Radiology,
The Perelman School of Medicine,
University of Pennsylvania,
Philadelphia, PA, USA

Introduction

Ureteropelvic junction (UPJ) obstruction is a relatively common cause of renal obstruction potentially causing renal damage by hindering urinary excretion due to narrowing at the junction of the renal pelvis and proximal ureter. The UPJ obstruction can be intrinsic, more common in younger children, or extrinsic and related to a crossing renal vessel, which is more frequent in older children [1]. Functional MR urography (fMRU) is a valuable tool for the morphological and functional evaluation of UPJ obstruction and other complex urinary tract abnormalities [2, 3]. Currently, no modality

Springer

provides a numeric threshold to differentiate patients with pelvicalyceal dilation due to UPJ obstruction requiring surgery from the ones that do not, or one that predicts renal function after surgery [4, 5]. Although there is still controversy on the criteria for selecting cases of UPJ obstruction going to surgery, widely accepted criteria include symptomatic patients, decreased renal function (i.e. unilateral obstruction with less than 40% of differential renal function on renography or fMRU, or bilateral UPJ obstruction with renal parenchymal atrophy, recurrent urinary tract infections and renal stones [6].

Diffusion tensor imaging (DTI) measures the orientation-dependent Brownian motion of water molecules to quantitatively assess the microstructure and morphology of different tissues in the body, including the kidney. Quantitative measurements from DTI include fractional anisotropy, which is a measure of the directional inequality of water molecule motion in a tissue, and apparent diffusion coefficient (ADC), a measure of the directionally averaged diffusivity [7]. Previous research showed that nephrons are well organized within the renal parenchyma and follow a radial arrangement [4, 8]. Recently, Li et al. [8] showed that DTI of renal allografts correlated with histopathological findings in a pediatric population. Few adult studies have found a direct relationship between fractional anisotropy values and estimated glomerular filtration rate (GFR) in native [9] and transplanted kidneys [10, 11]. In addition to voxel-wise measure of DTI parameters, tractography maps of the renal parenchyma and measures of mean track length and volume are obtained through additional algorithms by using an fractional anisotropy and an angular difference threshold between two adjacent voxels [7].

Our aim was to evaluate the feasibility of using DTI to identify UPJ obstruction kidneys and to evaluate the potential of renal DTI as a biomarker for quantifying renal disease in UPJ obstruction.

Materials and methods

Subjects

This retrospective study was approved by the institutional review board at our hospital and was performed in compliance with the Health Insurance Portability and Accountability Act (HIPAA). A waiver of informed consent was granted. fMRU studies with a UPJ obstruction configuration were identified using a picture and archiving communication system (PACS) search engine (Softek Illuminate; Softek Solutions, Prairie Village, KS). The radiology database was searched with the procedure description "MR UROGRAM W/3D" and the words "UPJO" or "Ureteropelvic" between January 2013 and October 2015. Based on previous published research, a DTI sequence is part of the routine clinical fMRU protocol to further evaluate obstructed and dysplastic kidneys [4].

Inclusion criteria for the fMRU were patient age between 0 and 18 years, UPJ obstruction that underwent pyeloplasty, and fMRU examination with 20-direction DTI with b-values of b=0 s/mm^2 and b=400 s/mm^2. In patients with unilateral UPJ obstruction, the contralateral anatomically normal kidney served as a control (n=7). In cases of bilateral UPJ obstruction or for subjects with a single kidney, an age-matched kidney from a normal fMRU study (n=2) or contralateral normal kidney in cases of ureterovesical junction obstruction (n=4) served as controls.

Excluded were subjects with no DTI sequence meeting the study inclusion criteria (b=0 s/mm^2 and b=400 s/mm^2, 20 directions, 1.5 Tesla [T]) (n=38) or technically limited DTI (n=13): 1) motion artifact, defined as transverse (red) tracks instead of vertical (blue) tracks in the rectus abdominis and psoas muscles (n=11), 2) superior half of UPJ obstruction kidney out of the field of view (n=1) and 3) subject with metallic spine rods (n=1). Additional criteria for exclusion were: 1) pyeloplasty before the fMRU study (n=8), 2) subjects with UPJ obstruction configuration not treated with pyeloplasty (n=2), 3) a subject who underwent nephrectomy following fMRU (n=1) and 4) an incomplete fMRU study (n=1).

For analysis, we included 19 subjects (Fig. 1) (13 males and 6 females) and 26 kidneys, 13 with UPJ obstruction configuration that required pyeloplasty for treatment after the fMRU and 13 age-matched anatomically normal kidneys. Six subjects had bilateral UPJ obstruction kidneys and seven had a unilateral UPJ obstruction kidney. None of the bilateral UPJ obstruction kidneys had bilateral pyeloplasty. The mean age of subjects included in the study (cases and controls) was 6.15 years (range: 0.39–17.45 years) and the median follow-up between fMRU and retrospective recollection of data was 360 days (range: 27–659 days).

Functional MR urography

Patients were prepared for fMRU following a standardized protocol [12, 13]. All patients received intravenous hydration before to imaging with 20 cc/Kg of normal saline infused over 30-40 min. Bladder catheterization was completed with either a Foley or a straight catheter that remained in place throughout imaging. Patients were imaged in a prone position. Fifteen min before intravenous contrast, 1 mg/Kg furosemide (maximum dose of 20 mg) was administered intravenously. All children younger than 7 years old were sedated.

Images were acquired with a 1.5-T MR system (Avanto; Siemens, Erlangen, Germany) using either a 6- or a 9-channel body matrix coil in combination with a 24-channel spine coil. The imaging protocol included the following pre-contrast sequences: sagittal half-Fourier acquisition single-shot spin-echo (HASTE) (repetition time [TR]/echo time [TE] 1,100/99 ms; slice thickness: 3 mm, matrix: 256 × 202), axial fat-suppressed T2-weighted image with motion reduction
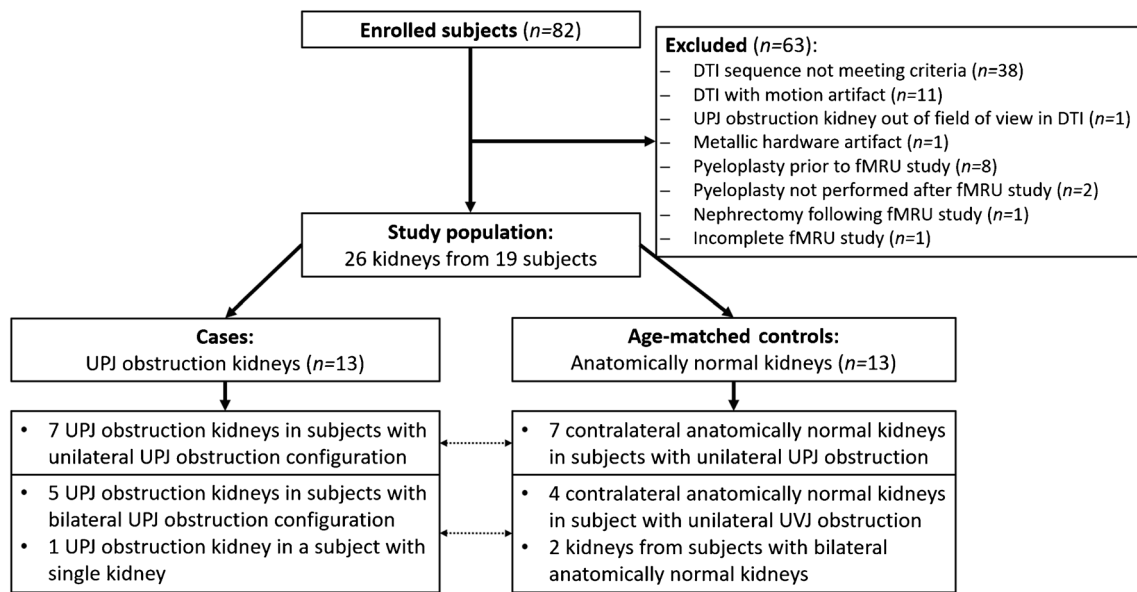
Fig. 1 Flow chart shows study population. *DTI* diffusion tensor imaging, *fMRU* functional magnetic resonance urography, *MRU* magnetic resonance urography, *UPJ* ureteropelvic junction, *UVJ* ureterovesicular junction

BLADE (TR/TE 6,000/145 ms; slice thickness: 3 mm, matrix: 320 × 320), coronal fat-suppressed 3-D T2-W sampling perfection with application-optimized contrasts using different flip angle evolution (SPACE) (TR/TE 1,800/599 ms; slice thickness: 1 mm, matrix: 256 × 168).

For functional analysis, pre- and post-contrast coronal fat-suppressed 3-D T1 gradient recalled echo (GRE) images with volumetric interpolated breath-hold examination (VIBE) (TR/TE 3.63/1.23 ms; slice thickness: 2-3 mm; matrix: 256 × 168, flip angle 30°) were performed. Dynamic sequences were repeated until contrast was seen in both ureters below the level of the lower pole of the kidney or up to 15 min with increasing pauses (2-42 s) between acquisitions. For post-contrast imaging, gadolinium-diethylenetriaminepentaacetic acid (DTPA) (Magnevist; Bayer-Schering, Berlin, Germany) at a dose of 0.2 ml/kg (0.1 mmol/Kg), with a minimum dose of 2 mL and a maximum dose of 20 mL, was administered at a slow rate of infusion. In selected cases, delayed post-contrast imaging was performed.

DTI of the abdomen was obtained using a fat-suppressed spin-echo echo-planar sequence (TR/TE 2,600-3,900/64-74 ms). A slice thickness of 4 mm, a matrix size of 128 × 96 and a bandwidth of 1,698 Hz/pixel were used. The field of view was 192 × 192 mm^2 (n=4), 256 × 256 mm^2 (n=12) or 384 × 384 mm^2 (n=3) depending on patient size. Diffusion gradients were applied in 20 non-collinear directions with b=400 s/mm^2. A volume without diffusion gradients (b=0 s/mm^2) was also acquired. Four averages were obtained for each sequence without respiratory triggering. We used selective fat suppression with spectral adiabatic inversion recovery and standard shimming was performed through pre-imaging with the Siemens diffusion sequence.

For all subjects, a parallel imaging acceleration factor of 2 was used.

Imaging evaluation

Imaging evaluation was performed by a postdoctoral fellow with 5 years in pediatric radiology research experience (J.D.). Pelvicalyceal dilation was assessed on the axial fat-saturated T2-W using an adapted version of the Society for Fetal Urology classification by Riccabona et al. [14, 15]. Grades 0, 1 and 2 were considered non-dilated pelvicalyceal systems, whereas grade 3 ("Marked dilation of the renal calyces and pelvis with reduced forniceal and papillary differentiation without parenchymal narrowing"), grade 4 ("Gross dilation of the collecting system with narrowing of the parenchyma") and grade 5 ("Extreme hydronephrosis with only a thin, membrane-like residual renal parenchymal rim") were considered dilated systems. Normal or decreased corticomedullary differentiation was also evaluated on the same sequence for each kidney. Decreased corticomedullary differentiation was defined as a decrease in the expected thickness of the renal medulla and decrease in the normal T2 signal intensity difference between the renal cortex and medulla with generalized low T2 signal intensity of the renal parenchyma. This finding occurs in the context of long-standing impaired renal drainage [16, 17].

Imaging post-processing

The Children's Hospital of Philadelphia functional magnetic resonance urography (CHOP fMRU) software (available at www.chop-fmru.com) was used for the functional MR

urography analysis [13]. Calyceal transit time (CTT), the time it takes for the contrast agent to go from the aorta into the calyces, and renal transit time (RTT), the time it takes for the contrast agent to go from the aorta to the ureter at the level of the lower renal pole, and the parenchymal volume were calculated for each kidney [12, 13].

For the DTI analysis and segmentation, we used software package Diffusion Toolkit version 0.6.4.1 and TrackVis version 0.6.0.1 (www.trackvis.org) [18]. Tractography was reconstructed using a deterministic fiber tracking algorithm with a minimum fractional anisotropy threshold of 0.10 and a maximum turning angle of 55° between two adjacent voxels based on published parameters for renal tractography [4]. A postdoctoral fellow with 5 years of experience in DTI research (J.D.) used TrackVis to draw regions of interest (ROIs) covering the entire volume of the renal parenchyma, excluding the collecting system by evaluating the diffusion-weighted images, ADC and fractional anisotropy maps (Fig. 2). These images were used to avoid problems of alignment related to patient motion in-between sequences. The ADC and fractional anisotropy values based on the ROI data, and the mean length and volume of the tracks based on the fiber track data, were exported. An additional ROI in the mid-axial plane of each kidney (Fig. 2) was drawn for qualitative evaluation of the scalar fractional anisotropy tractography maps.

The fiber tracks obtained from the ROIs were qualitatively analyzed for tractography quality, direction of tracks and differences in fractional anisotropy within the renal parenchyma. This assessment was done using two tractography maps: 1) a standard color-coded reconstruction to visualize the orientation of tracks where blue tracks represented diffusion in the craniocaudal direction, green tracks characterized diffusion in the anteroposterior direction and red tracks showed diffusion in the transverse direction, and 2) a scalar fractional anisotropy map with minimum and maximum fractional anisotropy thresholds of 0.1 and 0.6, respectively.

The extension of tracks following the psoas muscle or into adjacent organs (liver for the right kidney or spleen for left kidney) was recorded. The radial distribution of tracks was evaluated with a 3-point scale: 1) clear radial organization of fibers, 2) partial radial organization of fibers with random non-organized fibers and 3) non-radial organization pattern (Fig. 3). The corticomedullary differentiation on the scalar tractography fractional anisotropy maps was also assessed (Fig. 4).

Statistical analysis

Statistical analyses were performed using SPSS (version 20; IBM Corp., Armonk, NY). For the descriptive analysis, absolute distributions, percentages and means, standard deviations, medians and ranges were calculated. To evaluate differences in the distribution of nominal data the Fisher exact test and the Phi coefficient were used. The Mann-Whitney U test was used to compare age and different fMRU parameters between the groups. To evaluate the relationship of the different variables with age, linear regressions were performed. A Pearson correlation was used to correlate fMRU volumes and tractography volumes. A Wilcoxon test was calculated to find differences between volumes obtained by fMRU and DTI. Analysis of covariance (ANCOVA) controlling for age (a covariate) were used to compare the different DTI parameters between UPJ obstruction and normal kidneys. Statistical significance was accepted at $P<0.05$.

Results

The distribution of the ages and genders of the patients between those with UPJ obstruction and those with anatomically normal kidneys was similar. The mean age for UPJ obstruction patients was 7.07 years (range: 0.48–17.45 years) and for those with normal kidneys 7.33 years (range: 0.39–17.45 years) (Mann-Whitney U test, $P=0.80$) with 10 males and 3 females in the UPJ obstruction patients and 8 males and 5 females in the group with normal kidneys (Fisher exact test, $P=0.67$). Summary of the modified Society for Fetal Urology classification for grading of pelvicalyceal dilatation and the fMRU parameters are included in Table 1.

Evaluation of DTI

Failure rate The failure rate due to technical limitations of DTI was 13/26 (50%) in UPJ obstruction kidneys. This included motion artifact ($n=11$), UPJ obstruction kidney out of the field of view ($n=1$) and a subject with metallic spine rods ($n=1$).

Changes with age The ROI-based fractional anisotropy decreased with age for UPJ obstruction kidneys (change fractional anisotropy unit/year: -0.002; $P=0.032$) and normal kidneys (change fractional anisotropy unit/year -0.003; $P<0.001$), and the ROI-based ADC increased with age for normal kidneys (change ADC [mm²/s]/year: 3.54×10^{-5} mm²/s; $P<0.001$) but not for UPJ obstruction kidneys ($P=0.11$). The track volume increased for UPJ obstruction (change cm³/year: 9.59 cm³; $P=0.002$) and normal kidneys (change cm³/year: 10.7 cm³; $P<0.001$). Mean track length increased with age for both UPJ obstruction kidneys (change mm/year: 0.48 mm; $P<0.001$) and normal kidneys (change mm/year: 0.27 mm; $P=0.043$). For additional details, see Table 2.

There was a high correlation between the track volumes obtained by DTI and renal volumes on fMRU for UPJ obstruction kidneys ($R=0.81$; $P<0.001$) and for normal kidneys
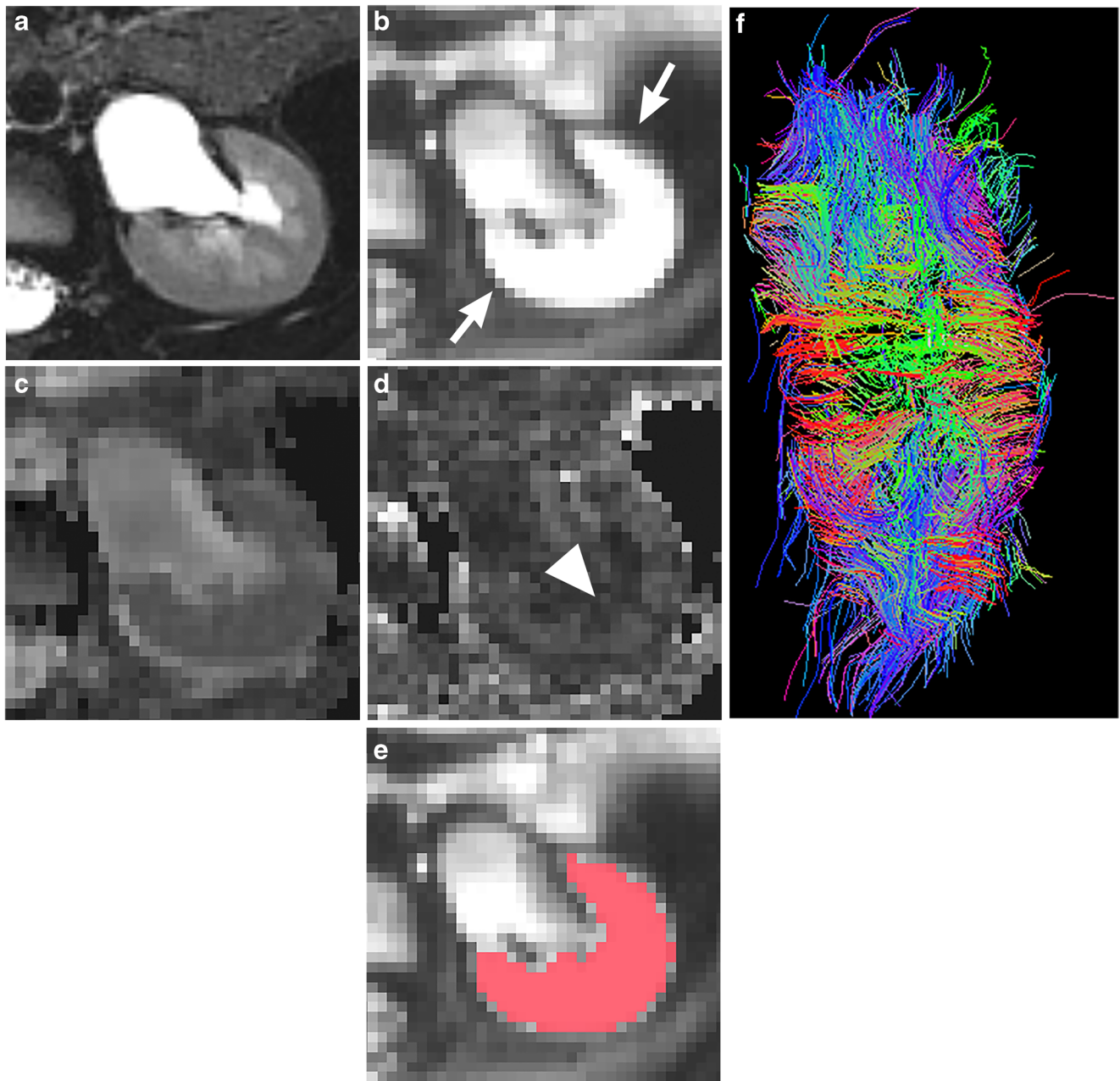
Fig. 2 Renal region of interest (ROI) placement in the left kidney of a 5.5-year-old boy with ureteropelvic junction obstruction. **a** Axial T2-W image shows grade 3 pelvicalyceal dilatation. **b** Axial diffusion-weighted (b=400 mm/s^2) image depicts the limits of the renal parenchyma (*arrows*). **c** Axial apparent diffusion coefficient map and (**d**) axial fractional anisotropy map used in conjunction with one another to avoid placing the ROI within the pelvicalyceal system. Note the corticomedullary differentiation in the fractional anisotropy map (*arrowhead*). Voxel dimensions for images (**b, c, d**) are 2 × 2.7 mm in plane with 4-mm section thickness and are used for placement of ROI only. **e** ROI placement is depicted in pink. **f** Coronal tractographic image of the post-processed kidney

(R=0.89; P<0.001). However, DTI measured volumes were significantly higher than fMRU measured volumes among both UPJ obstruction and normal kidneys. (Wilcoxon P=0.001). The median fMRU volume for UPJ obstruction and normal kidneys were 64.3 cc^3 and 75.4 cc^3, respectively, whereas the median DTI tractography volumes for UPJ obstruction and normal kidneys were 126.0 cm^3 and 115.9 cm^3, respectively.

Differences in DTI-based measurements between UPJ obstruction and normal kidneys

ANCOVA correcting for age was used to compare the different DTI parameters between UPJ obstruction kidneys and normal age-matched kidneys (Table 3). There were significant group differences in fractional anisotropy value and the track

Fig. 3 The grading of degree or track organization is illustrated on diffusion tensor imaging in three subjects. **a** Normal right kidney in a 5.5-year-old boy with clear radial distribution of tracks. **b** Left kidney with ureteropelvic junction (UPJ) obstruction and grade 4 pelvicalyceal dilatation in a 6.6-year-old boy with partial radial organization of fibers. **c** Left kidney with UPJ obstruction and grade 5 pelvicalyceal dilatation in a 12.4-year-old boy with non-radial organization of fiber tracks
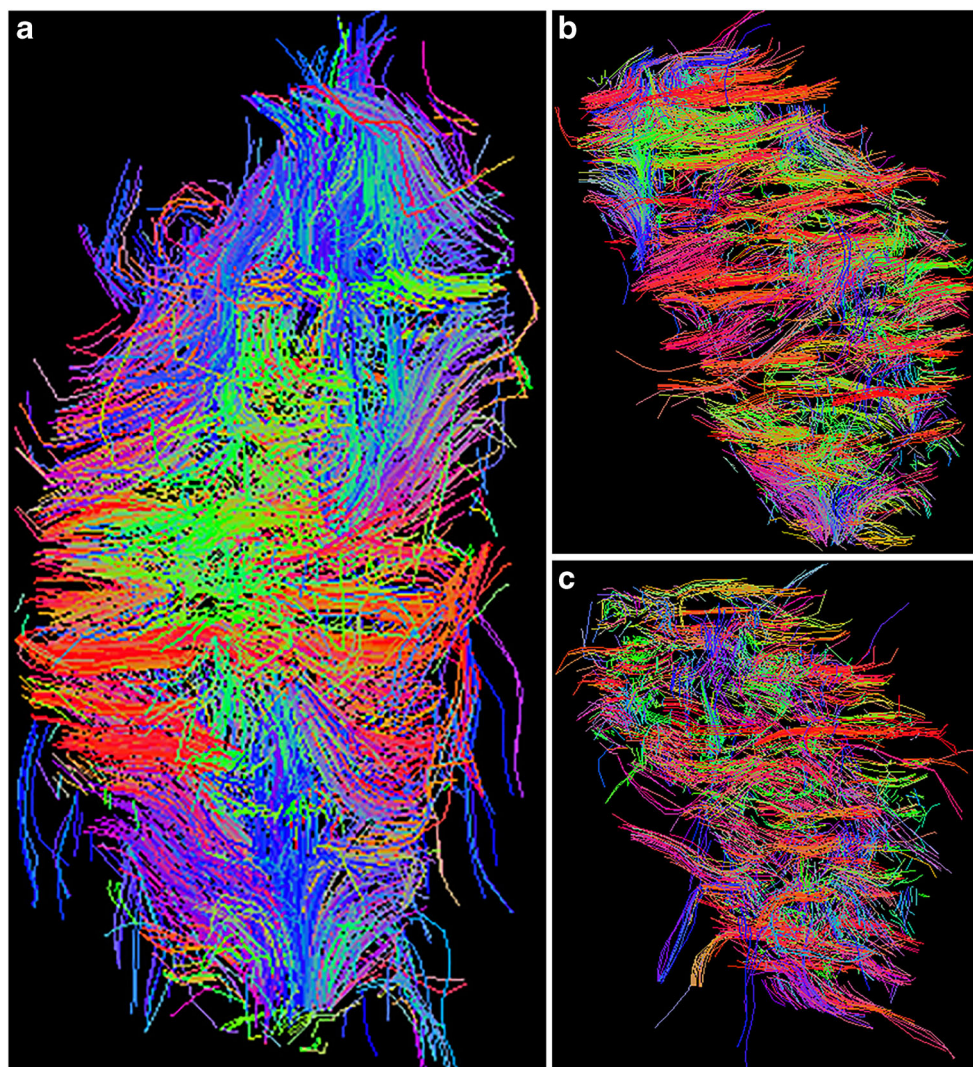
length (P=0.01) (Fig. 5). There was also a trend toward higher ADC in UPJ obstruction kidneys in comparison to normal kidneys, but statistical significance was not reached (P=0.062).

The corticomedullary differentiation on the scalar tractography fractional anisotropy maps showed a strong association with the corticomedullary differentiation seen on T2-W (Phi coefficient 0.843, P<0.001). There was agreement in the measurements of 24/26 kidneys (92%) (16/26 normal corticomedullary differentiation in both sequences and 8/26 with abnormal/decreased corticomedullary differentiation in both sequences). In 2/26 kidneys (8%), normal corticomedullary differentiation was seen on T2-W, but decreased corticomedullary differentiation was observed on the scalar tractography fractional anisotropy maps (Fig. 4). The evaluation of radial distribution of tracks is included in Table 4. Due to the sample size, no additional analysis was possible with this variable.

Tractography artifacts

Fiber extension followed the anatomy of the psoas muscle in 17/26 kidneys (65.4%) and into an adjacent organ, liver for the right kidney or spleen for the left kidney, in 4/26 kidneys (15.4%) (Fig. 6). Extension was not more common for UPJ obstruction kidneys in comparison to normal kidneys (Fisher exact test, P>0.99).

Discussion

In this study, we found a lower fractional anisotropy and a shorter mean track length within the renal parenchyma in kidneys with UPJ obstruction that underwent pyeloplasty following the fMRU in comparison to anatomically normal age-related kidneys.

DTI has been evaluated as a possible biomarker of renal function in renal disease. Many groups have found higher
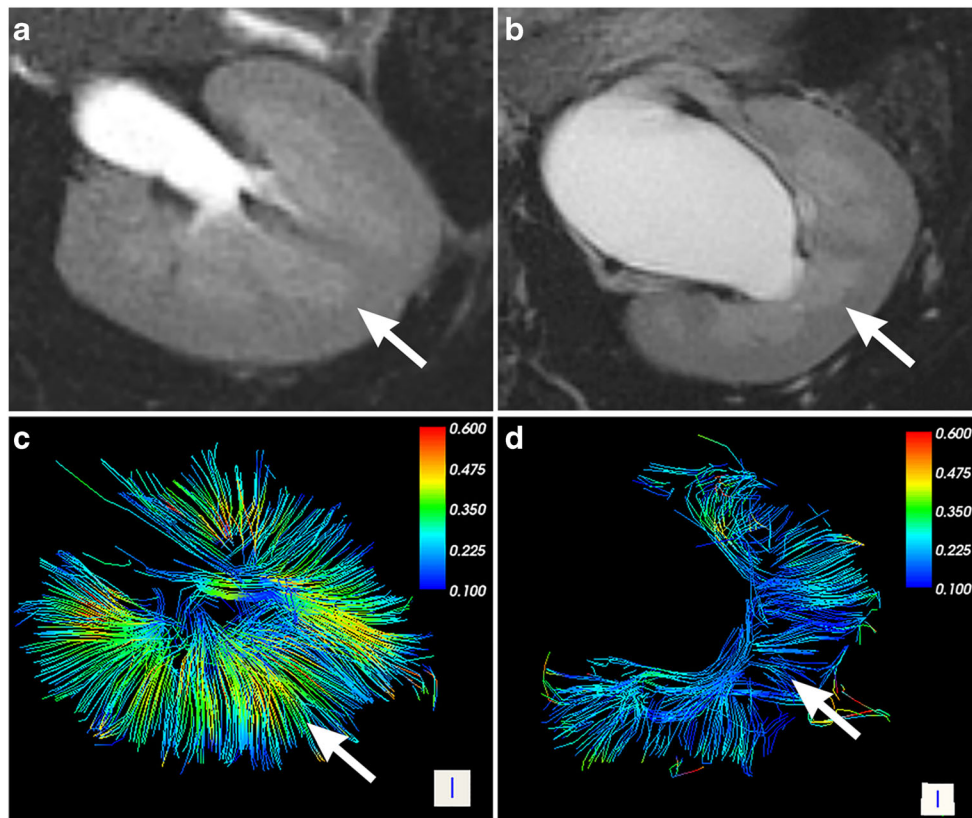
Fig. 4 Corticomedullary differentiation on the scalar tractography fractional anisotropy maps. **a** Normal left kidney in a 2.3-year-old boy with congenital hydronephrosis and suspicion of ureteropelvic junction (UPJ) obstruction. **b** Left kidney with UPJ obstruction in an 8.8-year-old boy with grade 3 pelvicalyceal dilatation. Note that on T2-W images the corticomedullary differentiation is still preserved for both patients (*arrows* in **a** and **b**). **c** Scalar fractional anisotropy tractography map of the patient in (**a**) shows an increased fractional anisotropy value at the location of the renal pyramids with maximum fractional anisotropy (*yellow* and *red*, *arrow*) in the center of the pyramids and relatively decreased fractional anisotropy values in the renal cortex (*blue*). **d** Scalar fractional anisotropy tractography map of the patient in (**b**) shows no clear differentiation of the renal cortex and medulla (*arrow*)

Table 1 Distribution of demographics, pelvicalyceal dilatation classification and functional magnetic resonance imaging parameters between kidneys with pyeloplasty due to ureteropelvic junction (UPJ) obstruction and age-related normal kidneys

	UPJ obstruction kidneys with pyeloplasty following MRI (n=13)	Normal kidneys (n=13)	P-value
Gender M/F	10/3	8/5	0.67
Mean age in years (range)	7.07 (0.48–17.45)	7.33 (0.39–17.45)	0.80
Modified SFU classification			
Grade 0	0	0	<0.001
Grade 1	0	4	
Grade 2	0	9	
Grade 3	2	0	
Grade 4	6	0	
Grade 5	5	0	
Functional MR urography			
Median CTT in seconds (range)	149 (109–359)	149 (89–265)	0.61
Median RTT in seconds (range)	209 (159–1,066)	149 (89–39)	0.002
Median volume in cm^3 (range)	64.27 (5–131)	75.41 (26–143)	0.19

CTT calyceal transit time, *F* female, *M* male, *RTT* renal transit time, *SFU* Society for Fetal Urology

Table 2 Relationship between the diffusion tensor imaging parameters and age for anatomically normal and ureteropelvic junction (UPJ) obstruction kidneys

	Kidney configuration	Relationship with age	R-square	Constant	B* (slope of age in years vs. diffusion tensor imaging parameter)	P-value
ROI-based FA	UPJ obstruction	Decrease	0.36	0.21	-0.002	0.032
	Normal	Decrease	0.56	0.24	-0.003	<0.001
ROI-based ADC (mm²/s)	UPJ obstruction	No significance	-	-	-	0.11
	Normal	Increase	0.69	0.002	3.54×10^{-5}	<0.001
Track volume (cm³)	UPJ obstruction	Increase	0.61	49.4	9.59	0.002
	Normal	Increase	0.95	40.5	10.7	<0.001
Mean track length (mm)	UPJ obstruction	Increase	0.72	8.46	0.48	<0.001
	Normal	Increase	0.32	13.4	0.27	0.043

ADC apparent diffusion coefficient, *FA* functional anisotropy, *ROI* region of interest

*B: values for the regression equation for predicting the dependent variable from the independent variable (i.e. change of diffusion tensor imaging parameter per year)

fractional anisotropy values of the renal medulla in comparison to the renal cortex [10, 19–22]. In our study, we avoided creating separate ROIs for the renal cortex and medulla. Although it is possible to differentiate the two structures on fractional anisotropy maps in non-dilated kidneys (Fig. 2), in our experience, this differentiation is no longer possible in most kidneys with pelvicalyceal dilatation grades 3 and 4 and in all kidneys with pelvicalyceal dilatation grade 5. There is a possibility that due to the smaller size of kidneys included in our study in comparison with adult kidneys, and due to the lack of respiratory triggering, the corticomedullary differentiation seen on the fractional anisotropy maps was lower in this study. Kataoka et al. [20] evaluated the effect of respiratory triggering and repeated breath holds for DTI of the kidneys in 16 healthy adults at 1.5 T. In their study, the use of repeated breath holds was inferior to respiratory triggering due to a lower corticomedullary differentiation, which they believe was related to the variation in position of the kidneys among the different breath holds [20]. Seif et al.

[23] used a multimodal non-rigid image registration algorithm and compared renal DTI with and without respiratory triggering in native and allograph kidneys. They found that registration improves the quality of DTI for both native and transplanted kidneys, but in native kidneys, respiratory triggering still provides a better quality of the different diffusion parameters [23]. In pediatric patients, respiratory triggering is challenging and the younger the child the more difficult it becomes. Due to the irregular and superficial respiration of most young pediatric patients, the use of bellows or navigator triggering is relatively inconsistent, making it very difficult to predict the scan time required to complete sequences [24]. Recently, Li et al. [8] showed satisfactory renal diffusion-weighted imaging with tractography with differentiation between the cortex and medulla in a pediatric population by using a patient free-breathing technique. However, the mean age of their subjects was 15.8 years [8]. The decreased corticomedullary differentiation on fractional anisotropy maps may be also related to the different pathophysiology of renal

Table 3 Analysis of covariance (ANCOVA) of the different diffusion tensor imaging parameters controlling for age

	Kidney configuration	Mean	Std. error	95% confidence interval	P-value
ROI-based FA*	UPJ obstruction	0.19	4.8×10^{-3}	0.18–0.20	0.001
	Normal	0.21	4.8×10^{-3}	0.20–0.22	
ROI-based ADC* (mm²/s)	UPJ obstruction	2.3×10^{-3}	8.2×10^{-5}	2.1×10^{-3}–2.5×10^{-3}	0.062
	Normal	2.1×10^{-3}	8.2×10^{-5}	1.9×10^{-3}–2.2×10^{-3}	
Tractography volume* (cm³)	UPJ obstruction	118.5	8.8	100.3–136.8	0.97
	Normal	117.9	8.8	99.7–136.3	
Mean track length* (mm)	UPJ obstruction	11.9	5.4	10.8–13.0	<0.001
	Normal	15.4	5.4	14.2–16.5	

ADC apparent diffusion coefficient, *FA* functional anisotropy, *ROI* region of interest, *UPJ* ureteropelvic junction, *Std error* standard error

*Covariates appearing in the model are evaluated at the age value of 7.21 years

Fig. 5 Scatterplot with linear regression shows the changes with age and between ureteropelvic junction (*UPJ*) obstruction kidneys and normal kidneys for (**a**) region of interest (*ROI*)-based fractional anisotropy (*FA*) and (**b**) mean track length
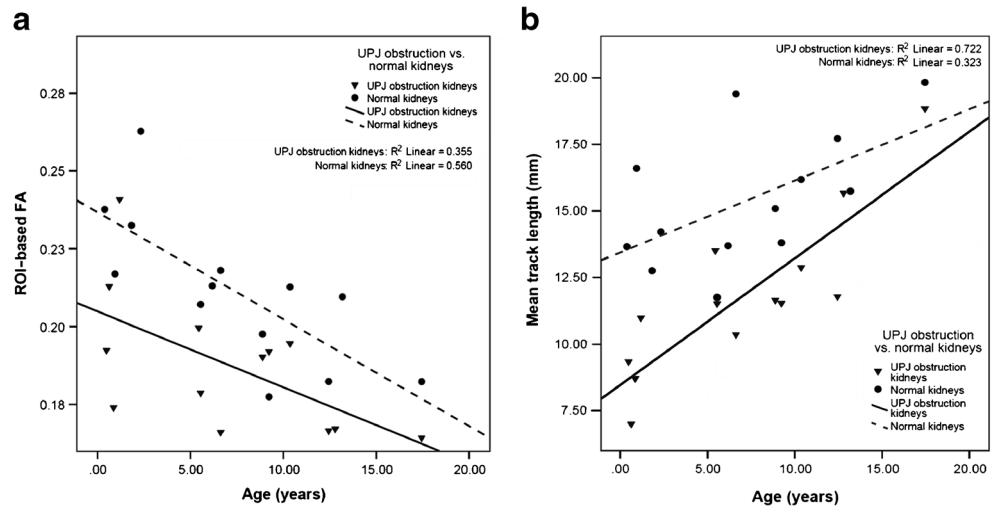
parenchymal injury of UPJ obstruction in comparison to renal allografts, the renal injury that has been most commonly evaluated with DTI [8, 10, 11]. The renal parenchyma in kidneys with UPJ obstruction kidneys is affected by pressure from post-renal obstruction due to ureteral intrinsic and extrinsic causes [25], which tend to affect the medulla before affecting the cortex. On the other hand, chronic injury to allografts is characterized by antibody-mediated and chronic active T cell-mediated rejection leading to formation of new basement membranes by endothelial cells, glomerular microvascular remodeling and arterial intimal fibrosis, which are primary renal cortical processes [26].

We were able to demonstrate a significant decrease in fractional anisotropy values, but we were only able to see a non-significant trend toward a higher ADC value in UPJ obstruction kidneys. This is in agreement with the findings of Hueper et al. [11], who found a 30% reduction in the fractional anisotropy value of the renal medulla in transplanted kidneys in comparison to healthy control kidneys, whereas the difference in the ADC value was about a 10% increase for the transplanted kidneys in relation to healthy control kidneys. They suggest that fractional anisotropy values may be a more sensitive parameter for detection of renal pathology [11]. Lanzman et al. [10] saw similar findings. An additional important consideration in evaluating ADC values is the significant differences in the ADC values measured in different studies mainly related to the different protocols used. Thus,

standardization of protocols used to measure ADC values is necessary if it is to be used as a functional renal marker [20]. On the contrary, based on renal DTI studies in adults, fractional anisotropy seems to be a more stable functional parameter [10, 21].

Our data also showed a high correlation between corticomedullary differentiation on scalar tractography fractional anisotropy maps and the corticomedullary differentiation on T2-W. In two subjects, changes were apparent on the scalar tractography fractional anisotropy map but not on T2-W. The opposite phenomenon did not happen in our small population. We hypothesized that changes in corticomedullary differentiation can be seen on DTI before they are evident on T2-W; however, this needs to be proven in a study with a larger sample size. Jaimes et al. [4] also found that abnormal moieties demonstrated poor corticomedullary differentiation of fractional anisotropy maps. They described loss of the radial arrangement of tracks on renal moieties with decreased renal function [4]. While our findings show a similar trend, our sample size limited the ability to elucidate additional conclusion on the tractography patterns on color-coded maps.

There is no standardized b-value for renal DTI with values ranging from 200 s/mm² to 700 s/mm² [4, 9, 19, 20, 22, 23]. Kataoka et al. [20] compared b-values of 200 s/mm² and 400 s/mm² finding that the latter one appears to be more consistent with lower standard deviation of the measurements and sufficient signal-to-noise ratio at 1.5 T. Multiple physiological

Table 4 Evaluation of radial distribution of tracks based on the color-coded tractography maps

	Ureteropelvic junction obstruction kidney (*n*=13)	Normal kidney (*n*=13)
Clear radial organization of fibers	5 (38.5%)	9 (69.2%)
Partial radial organization of fibers with random non-organized fibers	5 (38.5%)	3 (23.1%)
Non-radial organization pattern	3 (23.1%)	1 (7.7%)
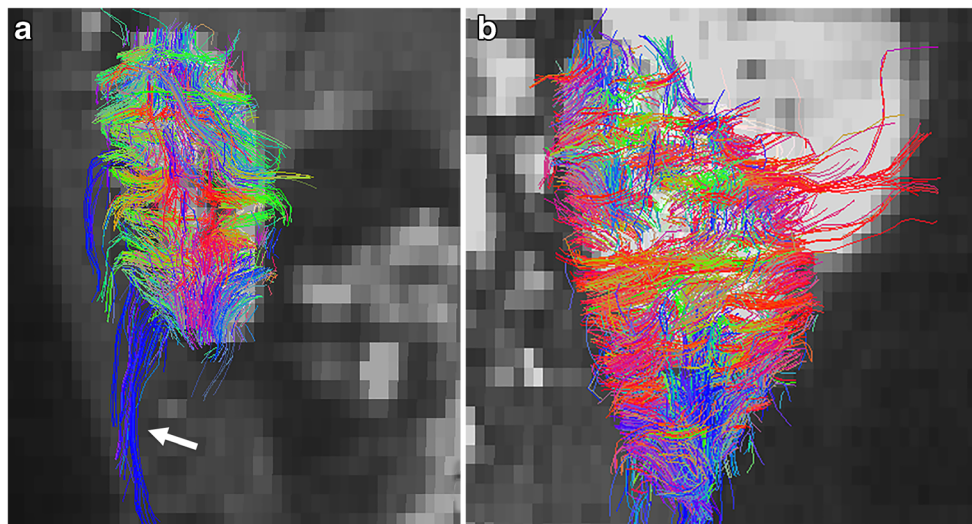
Fig. 6 Tractography artifacts. **a** Color-coded fiber tractography map overlaid on sagittal diffusion-weighted image (DWI) shows a normal kidney in a 1-year-old boy. Note the blue tracks following the normal anatomy of the psoas muscle (*arrow*). Fibers within the kidney depict a clear radial organization pattern. **b** Color-coded fiber tractography map overlaid on coronal DWI shows a kidney with ureteropelvic junction obstruction and grade III pelvicalyceal dilatation in a 6.2-year-old girl. Red tracks extend from the renal parenchyma into the spleen. Fibers within the kidney depict partial radial organization with some random non-organized fibers

factors may affect the motion of water in the kidneys including the flow along the tubules, flow in the arteries and veins, and transtubular flow from water reabsorption. The use of higher b-values decreases the intravoxel coherent motion related to perfusion seen at b-values below 200 s/mm^2 [4, 20]. The state of hydration may also have an influence on renal fractional anisotropy values [27]. As part of the standardized protocol for fMRU, all patients are hydrated at specific times before the MR imaging. We expect this protocol to control most of the differences related to flow in and along the tubules and from water reabsorption [4, 28].

Our data show that the tractography volume overestimates the renal parenchymal volume measured by fMRU. This finding was also described by Jaimes et al. [4]. With the low fractional anisotropy and high angular threshold used in this study for tractography, we saw tracks extending into the adjacent organs or following the psoas muscle in the majority of kidneys. Overestimation was equally common on anatomically normal and UPJO kidneys. The overestimation of tractography can be corrected up to a certain point by changing the tractography thresholds to a higher minimum fractional anisotropy value and a lower angular threshold. However, this modification negatively affects the number and concentration of tracks seen within the renal parenchyma and, thus, affects the evaluation of the tractography patterns (Figs. 3 and 4). A second option is to increase the image resolution, which decreases the volume averaging of the renal parenchyma. This modification impacts the scan time as well as the signal-to-noise ratio. The impact in the signal-to-noise ratio is expected to be marginal as the renal parenchyma has a high diffusivity with renal ADC values being about three times the ADC values of the brain [22].

It is important to realize that although the parenchyma may be evaluated with DTI, other factors affect the renal outcome of surgery. These include the different pathophysiology of UPJ obstruction in patients and surgery complications or failure [25, 29]. Some of the causes of UPJ obstruction are intrinsic, including ureteral scaring or incomplete recanalization during development and abnormal peristalsis of the ureter at the ureteropelvic junction related to muscular or neural changes; and extrinsic causes such as the presence of a crossing vessel, high insertion of the ureter at the renal pelvis or abnormal position or hypermobility of the kidney [25]. Crossing vessels, which are more common in older children with a late presentation, are also present in up to 25% of antenatal diagnosis of UPJ obstruction and are difficult to evaluate with fMRU as the dose of contrast and injection rate are for functional evaluation of the renal parenchyma instead of the renal vasculature [1]. Diffusion tensor imaging is not expected to add anything to their detection, mainly due to spatial resolution. Contrast-enhanced MR angiography may be better for the depiction of abnormality [30, 31]. In older patients, kidneys with UPJ obstruction due to a crossing vessel are expected to have good function as in most cases obstruction is intermittent [32]. In younger patients, the impact of renal function is still to be determined.

Limitations of this study include its retrospective nature and the sample size. Due to the thresholds used for tractography, tracks were detected extending into the adjacent organs and muscle in most patients. We avoided problems in data interpretation by not using track-based ADC and fractional anisotropy values as quantitative parameters and by doing qualitative evaluation of the tractography patterns. We used different fields of view for subjects, which affects the voxel

volume. Nevertheless, it is important to realize that pediatric patients have a variable size and using the same field of view for all patients would have had a negative effect on the visualization of relatively small organs in infants and younger children. Also, the protocol was done without respiratory triggering. This may be one of the leading causes for our high failure rate and may contribute to artifacts seen in the tractography maps. Serum creatinine was not routinely obtained in our institution; for this reason, we could not correlate renal ADC of fractional anisotropy values with GFR as done in several other studies in adults. Most pyeloplasties are performed in patients younger than 5 years of age and only four children in our study were below that threshold.

Conclusion

We demonstrated that fractional anisotropy is lower in UPJ obstruction than in normal kidneys. It is necessary to improve this technique to increase the success rate and to perform more studies to evaluate if a decrease in fractional anisotropy can differentiate UPJ obstruction kidneys from hydronephrotic kidneys without UPJ obstruction. We acknowledge this is a pilot study and we hope future research can evaluate DTI of children with kidney with UPJ obstruction configuration pre- and post-pyeloplasty.

Compliance with ethical standards

Conflicts of interest Dr. J. I. Berman is a consultant for McGowan Associates. Drs. Delgado, Maya, Back and Darge and technologist Carson have no disclosures.

References

1. Weiss DA, Kadakia S, Kurzweil R et al (2015) Detection of crossing vessels in pediatric ureteropelvic junction obstruction: clinical patterns and imaging findings. J Pediatr Urol 11:173 e171–173 e175
2. Dillman JR, Trout AT, Smith EA (2016) MR urography in children and adolescents: techniques and clinical applications. Abdom Radiol (NY) 41:1007–1019
3. Darge K, Higgins M, Hwang TJ et al (2013) Magnetic resonance and computed tomography in pediatric urology: an imaging overview for current and future daily practice. Radiol Clin North Am 51:583–598
4. Jaimes C, Darge K, Khrichenko D et al (2014) Diffusion tensor imaging and tractography of the kidney in children: feasibility and preliminary experience. Pediatr Radiol 44:30–41
5. Romao RL, Farhat WA, Pippi Salle JL et al (2012) Early postoperative ultrasound after open pyeloplasty in children with prenatal hydronephrosis helps identify low risk of recurrent obstruction. J Urol 188:2347–2353
6. Kogan BA (2013) Chapter 37. Disorders of the ureter &ureteropelvic junction. In: McAninch JW, Lue TF (eds) Smith & Tanagho's general urology, 18th edn. The McGraw-Hill Companies, New York
7. Hagmann P, Jonasson L, Maeder P et al (2006) Understanding diffusion MR imaging techniques: from scalar diffusion-weighted imaging to diffusion tensor imaging and beyond. Radiographics 26: S205–S223
8. Li Y, Lee MM, Worters PW et al (2017) Pilot study of renal diffusion tensor imaging as a correlate to histopathology in pediatric renal allografts. AJR Am J Roentgenol 208:1358–1364
9. Liu Z, Xu Y, Zhang J et al (2015) Chronic kidney disease: pathological and functional assessment with diffusion tensor imaging at 3T MR. Eur Radiol 25:652–660
10. Lanzman RS, Ljimani A, Pentang G et al (2013) Kidney transplant: functional assessment with diffusion-tensor MR imaging at 3T. Radiology 266:218–225
11. Hueper K, Gutberlet M, Rodt T et al (2011) Diffusion tensor imaging and tractography for assessment of renal allograft dysfunction-initial results. Eur Radiol 21:2427–2433
12. Delgado J, Bedoya MA, Adeb M et al (2015) Optimizing functional MR urography: prime time for a 30-minutes-or-less fMRU. Pediatr Radiol 45:1333–1343
13. Khrichenko D, Darge K (2010) Functional analysis in MR urography - made simple. Pediatr Radiol 40:182–199
14. Fernbach SK, Maizels M, Conway JJ (1993) Ultrasound grading of hydronephrosis: introduction to the system used by the Society for Fetal Urology. Pediatr Radiol 23:478–480
15. Riccabona M, Avni FE, Blickman JG et al (2008) Imaging recommendations in paediatric uroradiology: minutes of the ESPR workgroup session on urinary tract infection, fetal hydronephrosis, urinary tract ultrasonography and voiding cystourethrography, Barcelona, Spain, June 2007. Pediatr Radiol 38:138–145
16. Dickerson EC, Dillman JR, Smith EA et al (2015) Pediatric MR urography: indications, techniques, and approach to review. Radiographics 35:1208–1230
17. Grattan-Smith JD, Little SB, Jones RA (2008) Evaluation of reflux nephropathy, pyelonephritis and renal dysplasia. Pediatr Radiol 38: S83–105
18. Wang R, Benner T, Sorensen AG et al (2007) Diffusion Toolkit: A software package for diffusion imaging data processing and tractography. Proceedings of the 15th Meeting of the International Society for Magnetic Resonance in Medicine. International Society for Magnetic Resonance in Medicine, Berkley, California
19. Kido A, Kataoka M, Yamamoto A et al (2010) Diffusion tensor MRI of the kidney at 3.0 and 1.5 Tesla. Acta Radiol 51:1059–1063
20. Kataoka M, Kido A, Yamamoto A et al (2009) Diffusion tensor imaging of kidneys with respiratory triggering: optimization of parameters to demonstrate anisotropic structures on fraction anisotropy maps. J Magn Reson Imaging 29:736–744
21. Notohamiprodjo M, Glaser C, Herrmann KA et al (2008) Diffusion tensor imaging of the kidney with parallel imaging: initial clinical experience. Investig Radiol 43:677–685
22. Notohamiprodjo M, Dietrich O, Horger W et al (2010) Diffusion tensor imaging (DTI) of the kidney at 3 tesla-feasibility, protocol evaluation and comparison to 1.5 Tesla. Investig Radiol 45:245–254
23. Seif M, Mani LY, Lu H et al (2016) Diffusion tensor imaging of the human kidney: does image registration permit scanning without respiratory triggering? J Magn Reson Imaging 44:327–334
24. Darge K, Anupindi SA, Jaramillo D (2011) MR imaging of the abdomen and pelvis in infants, children, and adolescents. Radiology 261:12–29
25. Williams B, Tareen B, Resnick MI (2007) Pathophysiology and treatment of ureteropelvic junction obstruction. Curr Urol Rep 8: 111–117
26. Hara S (2016) Current pathological perspectives on chronic rejection in renal allografts. Clin Exp Nephrol 21:943–951

27. Chandarana H, Lee VS (2009) Renal functional MRI: are we ready for clinical application? AJR Am J Roentgenol 192:1550–1557

28. Sigmund EE, Vivier PH, Sui D et al (2012) Intravoxel incoherent motion and diffusion-tensor imaging in renal tissue under hydration and furosemide flow challenges. Radiology 263:758–769

29. Tubre RW, Gatti JM (2015) Surgical approaches to pediatric ureteropelvic junction obstruction. Curr Urol Rep 16:72

30. Calder AD, Hiorns MP, Abhyankar A et al (2007) Contrast-enhanced magnetic resonance angiography for the detection of crossing renal vessels in children with symptomatic ureteropelvic junction obstruction: comparison with operative findings. Pediatr Radiol 37:356–361

31. Renjen P, Bellah R, Hellinger JC et al (2010) Pediatric urologic advanced imaging: techniques and applications. Urol Clin North Am 37:307–318

32. Rigas A, Karamanolakis D, Bogdanos I et al (2003) Pelvi-ureteric junction obstruction by crossing renal vessels: clinical and imaging features. BJU Int 92:101–103